

## **Electronic supplementary information**

# **Thienothiophene-based covalent organic frameworks as photocatalysts for visible light-triggered oxidation of sulfides to sulfoxides**

Keke Zhang, Kanghui Xiong, Fengwei Huang, Xiaoyun Dong, Bing Zeng, and Xianjun Lang\*

*Hubei Key Lab on Organic and Polymeric Optoelectronic Materials, College of  
Chemistry and Molecular Sciences, Wuhan University, Wuhan 430072, China.*

\*To whom correspondence should be addressed (Prof. X. J. Lang). E-mail address:

[xianjunlang@whu.edu.cn](mailto:xianjunlang@whu.edu.cn).

## Materials and methods

**Reagent:** Commercially available materials were purchased from Sigma-Aldrich, TCI, Adamas, etc. All commercially available reagents and solvents were used without further purification.

**Elemental analysis** was performed on an Elementar UNICUBE analyzer with CHNS model.

**Fourier transform infrared (FTIR)** spectra were recorded from 400 to 4000  $\text{cm}^{-1}$  on Nicolet 5700 FTIR Spectrometer by using KBr pellets.

**Nuclear magnetic resonance (NMR)** spectroscopy was utilized to decode the structural information of COFs at the molecular level by using a Bruker AVANCE III HD S6 400MHz NMR spectrometer at room temperature.

**Nitrogen sorption isotherm** and specific surface areas were determined at 77 K using a Micromeritics ASAP 2460 automated system with the Brunauer–Emmet–Teller (BET) method, the samples were degassed in a vacuum ( $< 1 \times 10^{-5}$  bar) at 100 °C for 6 h in the Micromeritics system before  $\text{N}_2$  physisorption.

**Scanning electron microscopy (SEM)** images were measured on a Zeiss Merlin Compact running at the acceleration voltage between 0.1 and 20.0 kV.

**Powder X-ray diffraction** (PXRD) measurement was carried out adopting a Rigaku/Miniflex 600 diffractometer with a filtered Cu K $\alpha$  line, and the spectrum was gathered from 2 to 30° at room temperature.

**Transmission electron microscopy** (TEM) of COFs were estimated on a FEI Tecnai F20 operating at an accelerating voltage of 200.0 kV, respectively.

**Photoluminescence** (PL) spectra were obtained with an FLS1000 spectrophotometer.

With BaSO $_4$  as a reflectance standard.

**UV–visible diffuse reflectance spectra** of COFs were estimated from 300–800 nm by a UV–3600 UV-vis spectrophotometer (Shimadzu, Japan) configured with a diffuse reflectance measurement accessory.

**Thermogravimetric analysis** (TGA) spectra were recorded on an SDT Q600 thermogravimeter from 30 to 800 °C at a rate of 15 °C min $^{-1}$  under an atmosphere of N $_2$ .

**Electron paramagnetic resonance** (EPR) spectra were collected on a JEOL, JES-FA300 EPR spectrometer.

**Density functional theory** (DFT) calculations were carried out using the Gaussian 16W program package. Gaussian View 6.0 was used for the visualization. In short, the simplified unit consisting of TT-TAPB-COF and TT-TAPT-COF was taken into consideration. Molecular geometries were optimized using B3LYP/6-31G (d).

Subsequently, the optimized structures were implemented for B3LYP/6-31G (d,p) single point energy calculations. Hence, all calculations were corrected by the zero-point energy.

**Conversion of sulfides and selectivity of sulfoxides were defined as follows:**

$$\text{Conv. (\%)} = [(C_0 - C_S) / C_0] \times 100$$

$$\text{Sel. (\%)} = [C_p / (C_0 - C_S)] \times 100$$

where  $C_0$  is the initial concentration of sulfides, and  $C_S$  and  $C_p$  are the concentrations of sulfides and sulfoxides, respectively, at a certain time during the reaction.

**Electrochemical measurements:** A three-electrode electrochemical cell with an electrochemical workstation was employed to conduct experiments on a Metrohm Autolab PGSTAT302N. At first, the ultrasonic device dispersed 6 mg of TT-TAPB-COF and TT-TAPT-COF in 3 mL of 0.2 wt% Nafion respectively. Subsequently, the mixtures were dripped on glasses coated by indium tin oxide, that were adhered to a glassy carbon surface to serve as the working electrode, and the mixtures were repeatedly dropped and dried under illumination. The Ag/AgCl electrode and platinum wire functioned as the reference electrode and counter electrode, respectively, with 0.1 M  $\text{Na}_2\text{SO}_4$  aqueous solution as the electrolyte. Meanwhile, the four blue LEDs positioned at 2 cm from the photoelectrochemical cell were employed as the light source. The photocurrent densities were measured while being exposed to blue LEDs

with a scan rate of  $100 \text{ mV s}^{-1}$  and a time interval of 30 s. In total darkness, the Mott–Schottky plots were carried out upon frequencies of 500, 1000, and 1500 Hz, respectively. In addition, the electrochemical impedance spectroscopy (EIS) was performed under darkness at a bias potential of +1.5 V. Tetrabutylammonium hexafluorophosphate ( $\text{TBAPF}_6$ ) dissolving in anhydrous  $\text{CH}_3\text{CN}$ , was employed as the supporting electrolyte in cyclic voltammetry (CV) curves with a sweep rate of  $50 \text{ mV s}^{-1}$ . Meanwhile, the ferrocene/ferrocenium redox couple ( $\text{Fc}/\text{Fc}^+$ ) was utilized to properly calibrate the potential of the  $\text{Ag}/\text{AgCl}$  reference electrode.

**Construction of TT-TAPB-COF:** TT (0.15 mmol, 31.0 mg) and TAPB (0.10 mmol, 35.9 mg) were weighed into a Pyrex tube with a component solvent of benzyl alcohol/mesitylene (3 mL,  $v/v = 1/1$ ). The mixture was sonicated for 10 min, and then 300  $\mu\text{L}$  of 6 M acetic acid was added as a catalyst. Subsequently, the Pyrex tube was flame-sealed after degassing by freeze–pump–thaw three times. The tube was placed in a  $120 \text{ }^\circ\text{C}$  oven for 3 d. The product was collected via filtering separation and washed several times by methanol and acetone, after cooling down to room temperature. Then, the sample was further purified with acetone by Soxhlet extraction overnight. Finally, TT-TAPB-COF were dried at  $80 \text{ }^\circ\text{C}$  for 12 h under vacuum, to obtain deep-yellow powder.

**Construction of TT-TAPT-COF:** According to the above procedure, TT (0.15 mmol, 31.0 mg), TAPT (0.10 mmol, 36.2 mg), and component solvent of benzyl

alcohol/mesitylene (3 mL, v/v = 1/1) were used and TT-TAPT-COF was collected as deep-orange powder.

**The typical operation for the aerobic oxidation of sulfides:** A Pyrex reactor was filled with methanol (CH<sub>3</sub>OH, 1 mL), sulfide (0.3 mmol), and COFs (5 mg), followed by stirring under darkness for 15 minutes. Then, 0.1 MPa of O<sub>2</sub> was introduced into the sealed reactor. At room temperature, magnetic stirring and 460 nm blue LED irradiation induced this reaction. After centrifugating to remove the solid, gas chromatography with flame ionization detection (GC–FID) was employed to evaluate the supernatant. Through the utilization of gas chromatography–mass spectrometry, the components in the supernatant were verified in detail. The conversions of sulfide and the selectivity of the corresponding sulfoxide were determined by GC–FID using bromobenzene as the internal standard.

## Supplementary Figures and Tables

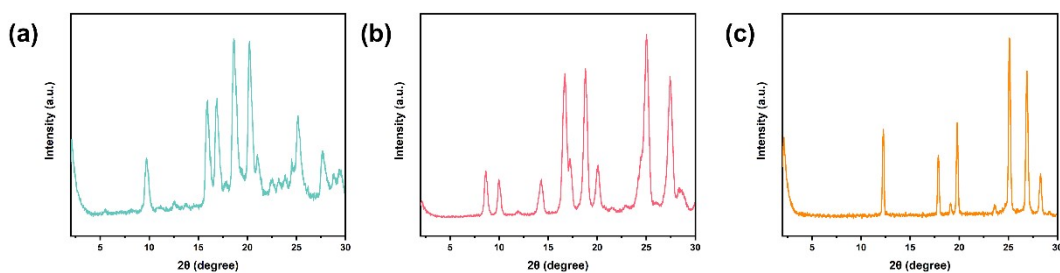


**Fig. S1.** PXRD measurements of TAPB (a), TAPT (b), and TT (c).

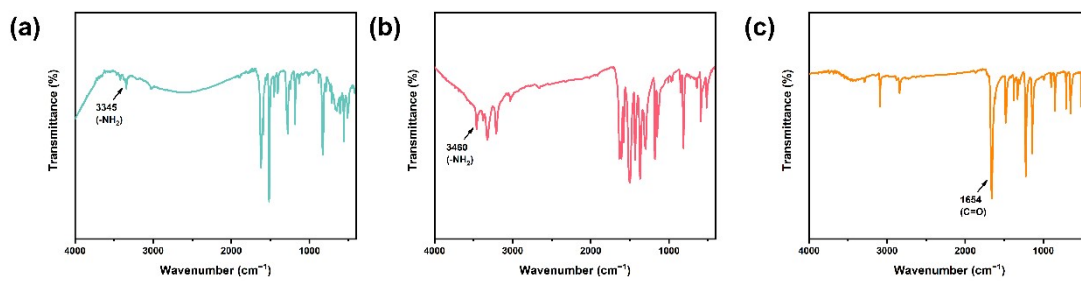


**Fig. S2.** FTIR spectra of TAPB (a), TAPT (b), and TT (c).

**Table S1.** Elemental analysis of TT-TAPB-COF and TT-TAPT-COF.

		N (%)	C (%)	H (%)	S (%)
TT-TAPB-COF	Measured	6.50	71.47	4.08	14.80
	Expected	6.89	72.87	4.46	15.77
TT-TAPT-COF	Measured	13.34	64.61	3.55	14.94
	Expected	13.71	66.64	3.95	15.70

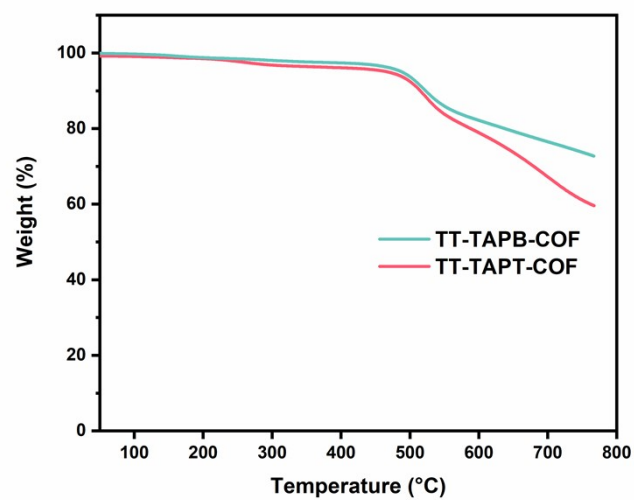


**Fig. S3.** The TGA curves of TT-TAPB-COF and TT-TAPT-COF.

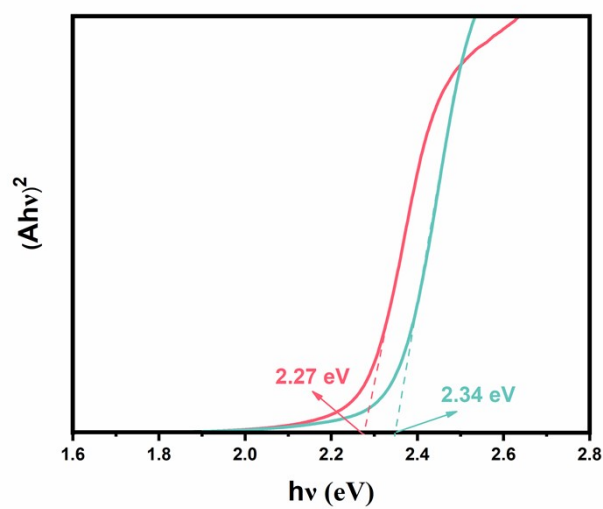


**Fig. S4.** The Tauc plots of TT-TAPB-COF and TT-TAPT-COF.



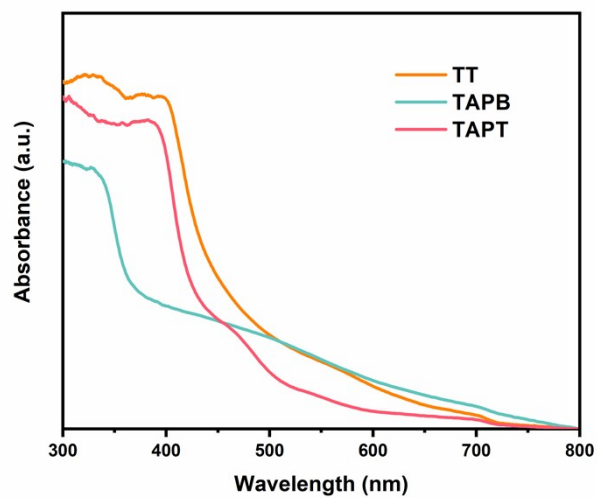


**Fig. S5.** The UV-visible DRS spectra of the building blocks of TT, TAPB, and TAPT.

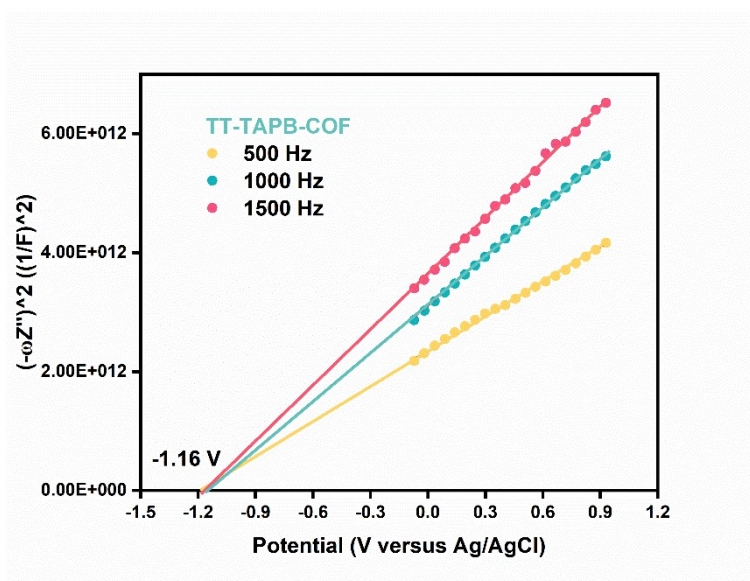


**Fig. S6.** The Mott-Schottky plots of TT-TAPB-COF.

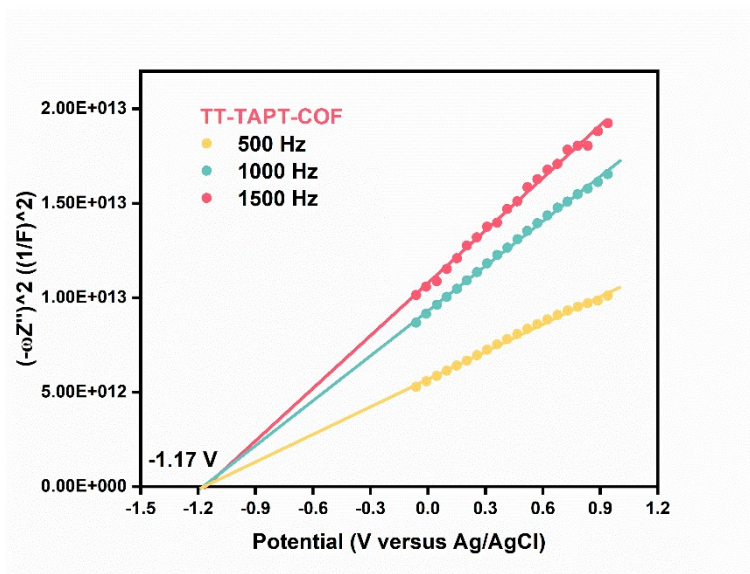


**Fig. S7.** The Mott–Schottky plots of TT-TAPB-COF.

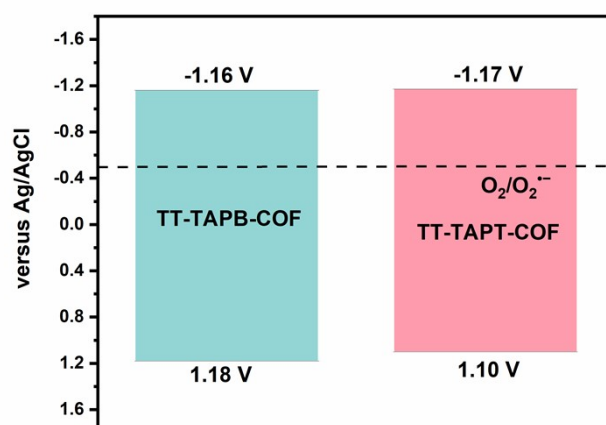


**Fig. S8.** The band structures of TT-TAPB-COF and TT-TAPT-COF.

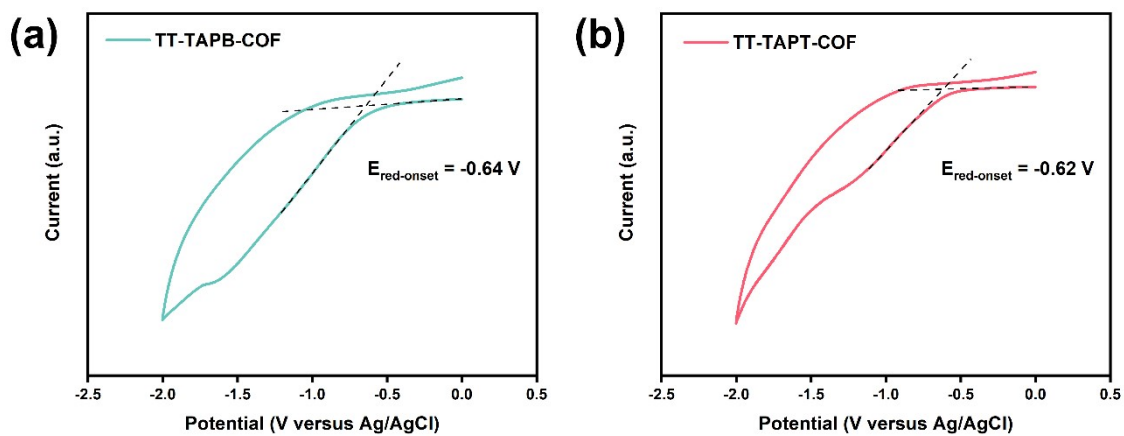


**Fig. S9.** The CV curves of TT-TAPB-COF (a) and TT-TAPT-COF (b).

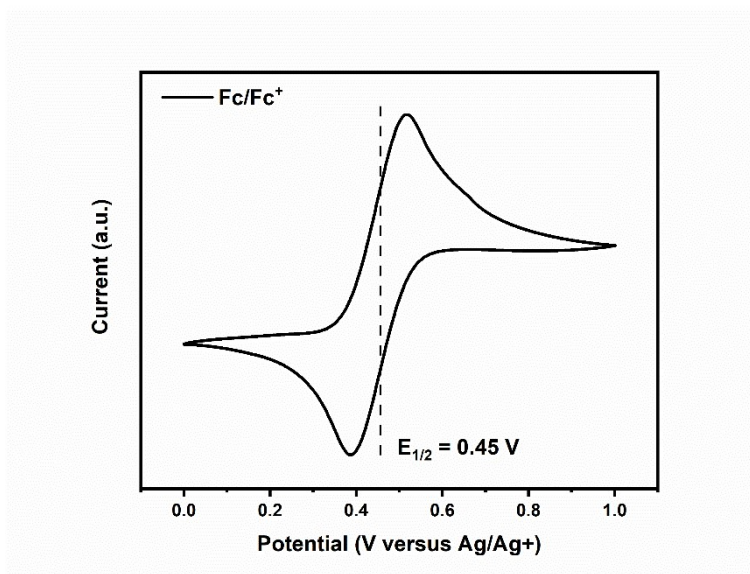


**Fig. S10.** The CV measurements of Fc/Fc<sup>+</sup> couple to calibrate the pseudo reference electrode.

**Table S2.** The performance of the building blocks on the blue light-triggered oxidation of methyl phenyl sulfide to methyl phenyl sulfoxide.<sup>a</sup>

Entry	Building block	Conv. (%) <sup>b</sup>	Sel. (%) <sup>b</sup>
1	TT	12	99
2	TAPB	0	--
3	TAPT	0	--

<sup>a</sup>Reaction conditions: methyl phenyl sulfide (0.3 mmol), photocatalyst (5 mg), blue LEDs (460 ± 10 nm, 3 W × 4), O<sub>2</sub> (0.1 MPa), CH<sub>3</sub>OH (1 mL), 2 h.

<sup>b</sup>Determined by GC–FID using bromobenzene as the internal standard.

**Table S3.** The influence of various solvents on the blue light-triggered oxidation of methyl phenyl sulfide to methyl phenyl sulfoxide.<sup>a</sup>

Entry	Solvent	Conv. (%) <sup>b</sup>	Sel. (%) <sup>b</sup>
1	CH <sub>3</sub> CN	57	99
2	C <sub>2</sub> H <sub>5</sub> OH	64	99
3	CH <sub>3</sub> OH	71	99

<sup>a</sup>Reaction conditions: methyl phenyl sulfide (0.3 mmol), photocatalyst (5 mg), blue LEDs (460 ± 10 nm, 3 W × 4), O<sub>2</sub> (0.1 MPa), solvent (1 mL), 2 h.

<sup>b</sup>Determined by GC–FID using bromobenzene as the internal standard.

**Table S4.** Comparison of the oxidation of methyl phenyl sulfide to methyl phenyl sulfoxide over various photocatalysts.

Entry	Photocatalysts	Conditions	t (h)	Conv. (%)	Sel. (%)	Ref.
1	AQ-COF (10 mg)	Sulfide (0.3 mmol), CH <sub>3</sub> CN (2 mL), Xe lamp (300 W, $\lambda = 400\text{--}780$ nm), O <sub>2</sub> (1 atm)	3	99	97	[1]
2	C-CMP (20 mg)	Sulfide (1.0 mmol), CH <sub>3</sub> CN (2 mL), Xe lamp (250 W), O <sub>2</sub> (1 atm)	8	99	93	[2]
3	Oxidized g-C <sub>3</sub> N <sub>4</sub> (5 mg)	Sulfide (0.5 mmol), CH <sub>3</sub> CN (2 mL), Xe lamp (50 W), O <sub>2</sub> (1 atm)	8	99	99	[3]
4	Zr-MOF-OH (7 mg)	Sulfide (0.2 mmol), CF <sub>3</sub> CH <sub>2</sub> OH (3.0 mL), white LED (5 W), O <sub>2</sub> (1 atm)	8	99	95	[4]
5	TiO <sub>2</sub> (40 mg)	Sulfide (0.3 mmol), amine additive (0.3 mmol), CH <sub>3</sub> OH (5 mL), Xe lamp (300 W, $\lambda > 400$ nm), O <sub>2</sub> (0.1 MPa)	5	99	99	[5]
6	COF-NUST-31 (4 mg)	Sulfides (0.1 mmol), CH <sub>3</sub> CN (1.5 mL), 30 W blue light ( $\lambda = 455\text{--}460$ nm), O <sub>2</sub> (1 atm)	4	99	98	[6]
7	TT-TAPT-COF (5 mg)	Sulfide (0.3 mmol), CH <sub>3</sub> OH (1 mL), blue LEDs (460 $\pm$ 10 nm, 3 W $\times$ 4), O <sub>2</sub> (0.1 MPa), rt	2.3	94	99	This work

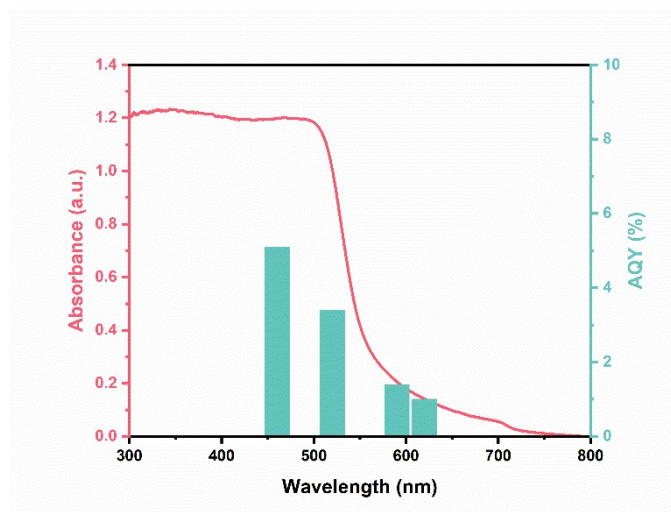


**Fig. S11.** The UV–visible diffuse reflectance spectrum of TT-TAPT-COF and the AQY under the irradiation of different wavelength light.

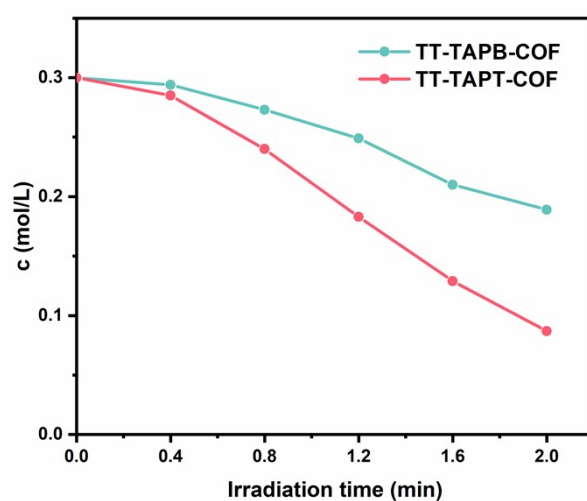


**Fig. S12.** The kinetic curves of TT-TAPB-COF and TT-TAPT-COF for the blue light-triggered oxidation of methyl phenyl sulfide to methyl phenyl sulfoxide. Reaction conditions: methyl phenyl sulfide (0.3 mmol), COF (5 mg), blue LEDs ( $460 \pm 10$  nm,  $3 \text{ W} \times 4$ ),  $\text{O}_2$  (0.1 MPa),  $\text{CH}_3\text{OH}$  (1 mL).

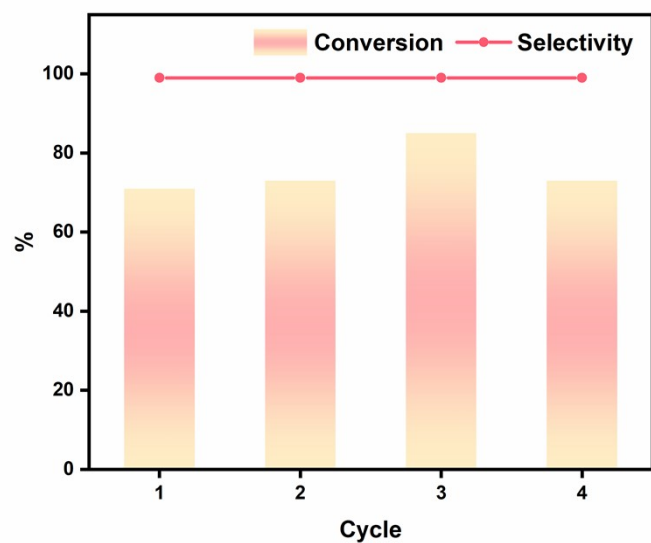


**Fig. S13.** The recyclability of TT-TAPT-COF photocatalyst for the blue light-triggered oxidation of methyl phenyl sulfide to methyl phenyl sulfoxide. Reaction conditions: methyl phenyl sulfide (0.3 mmol), TT-TAPT-COF (5 mg), blue LEDs ( $460 \pm 10$  nm,  $3 \text{ W} \times 4$ ),  $\text{O}_2$  (0.1 MPa),  $\text{CH}_3\text{OH}$  (1 mL), 2 h.

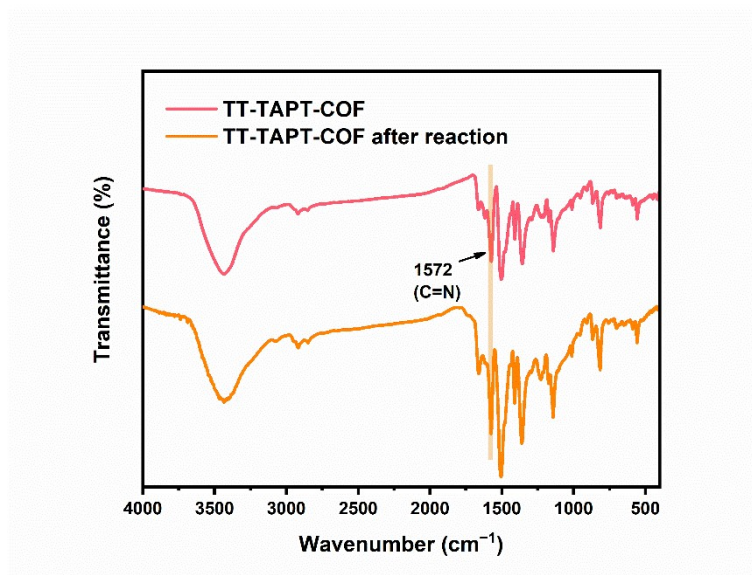


**Fig. S14.** FTIR spectra of the fresh TT-TAPT-COF and the collected TT-TAPT-COF after reaction.

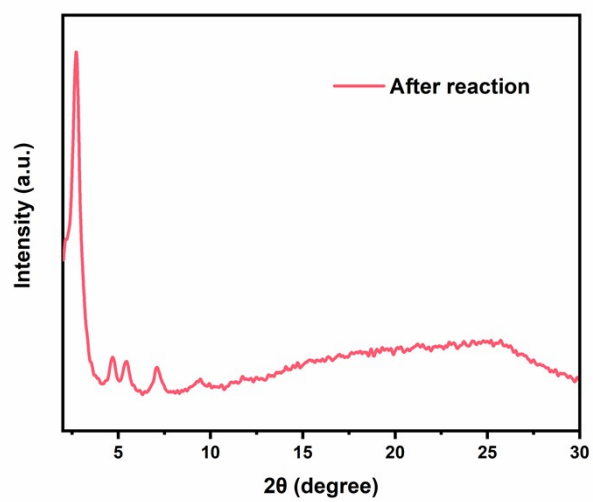


**Fig. S15.** The PXRD pattern of the collected TT-TAPT-COF after reaction.



**Fig. S16.** GC-FID results for Table 2.

Table 2, Entry 1

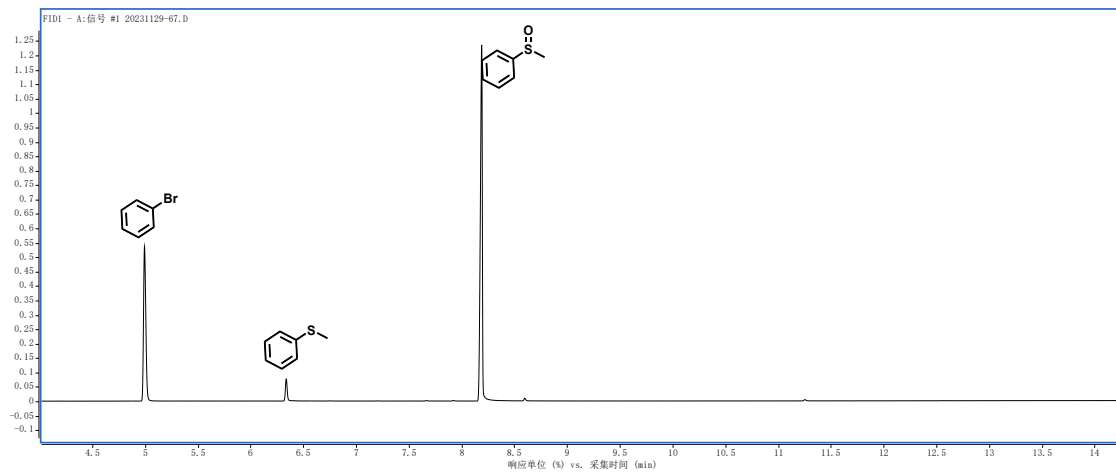


Table 2, Entry 2

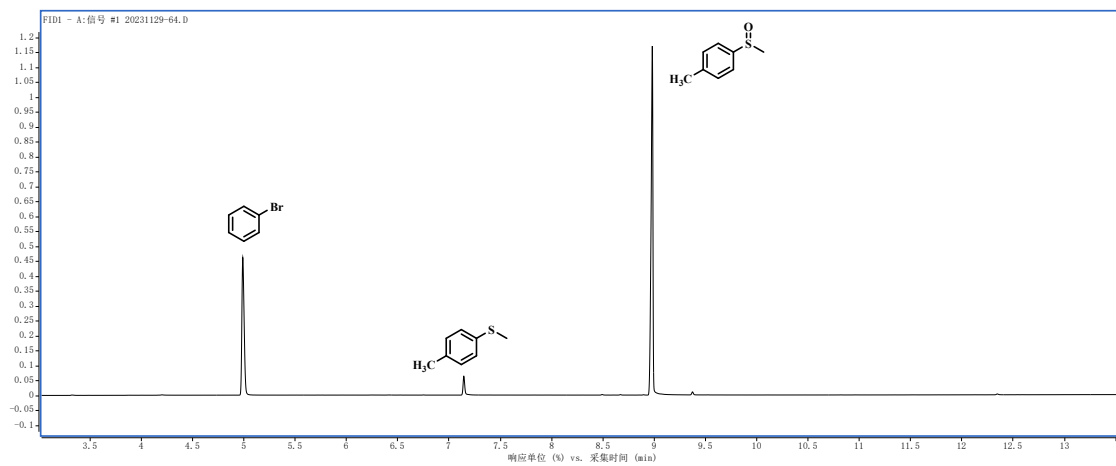


Table 2, Entry 3

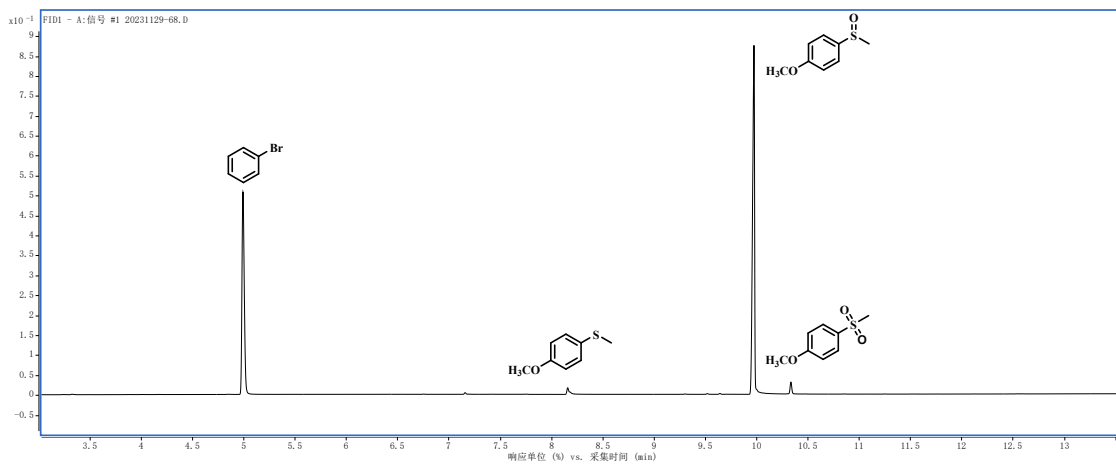


Table 2, Entry 4

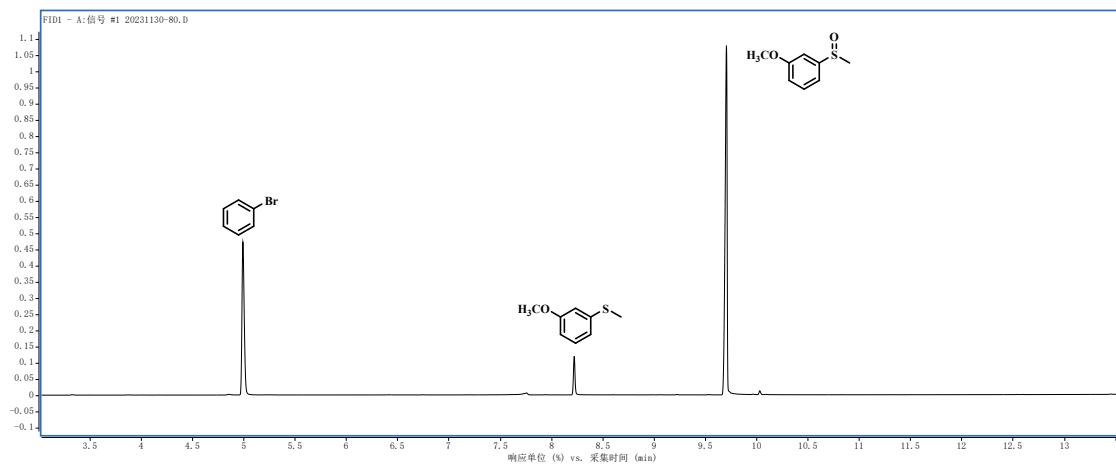


Table 2, Entry 5

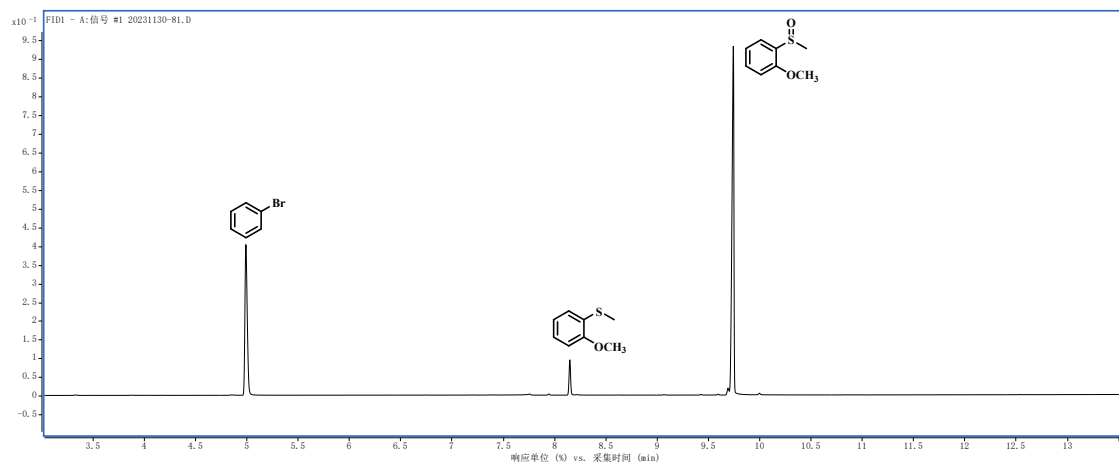


Table 2, Entry 6

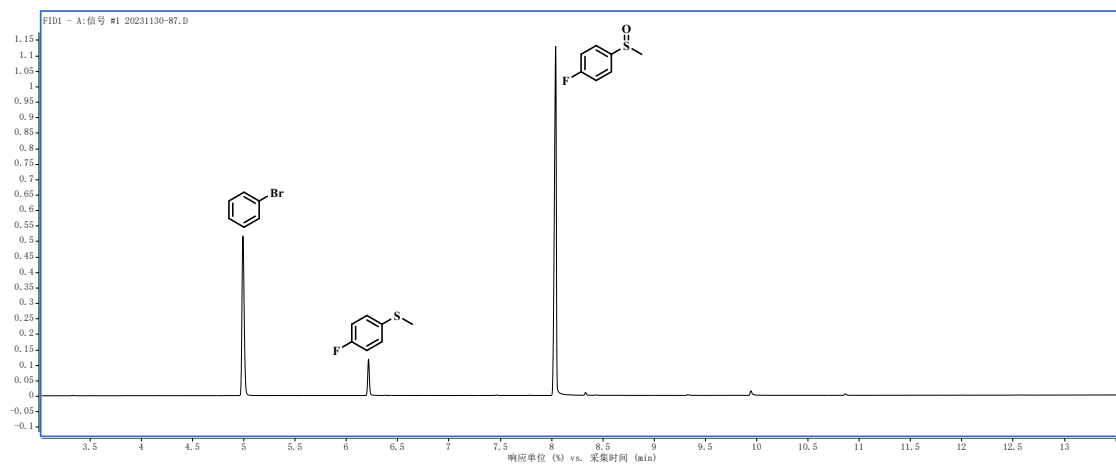


Table 2, Entry 7

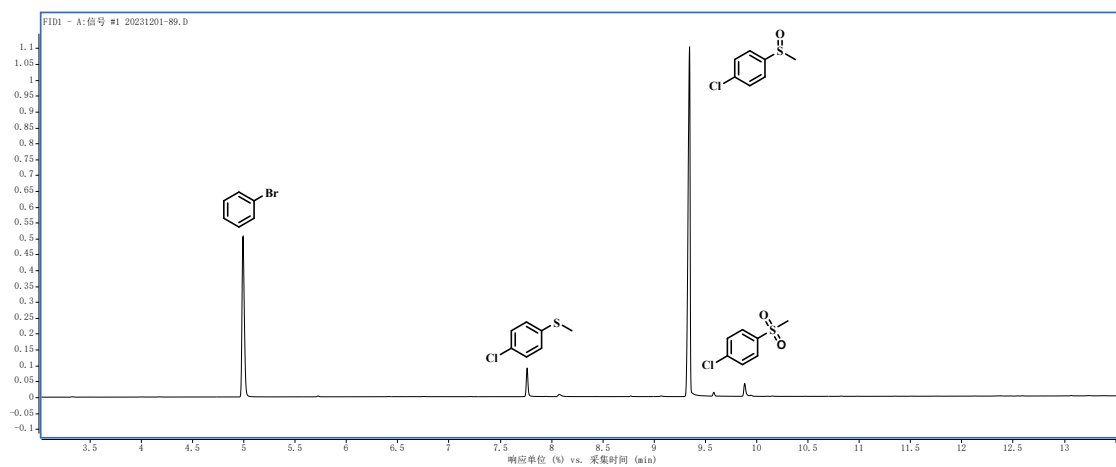


Table 2, Entry 8

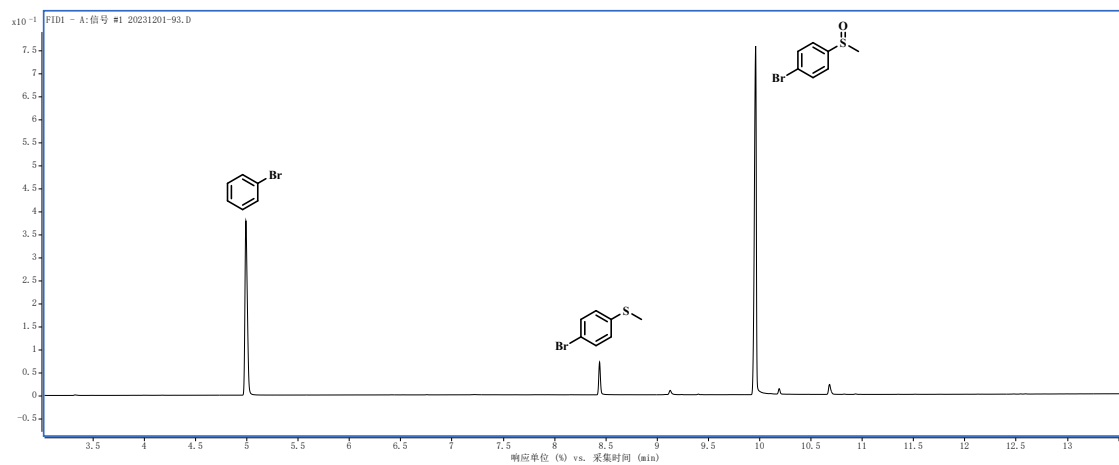


Table 2, Entry 9

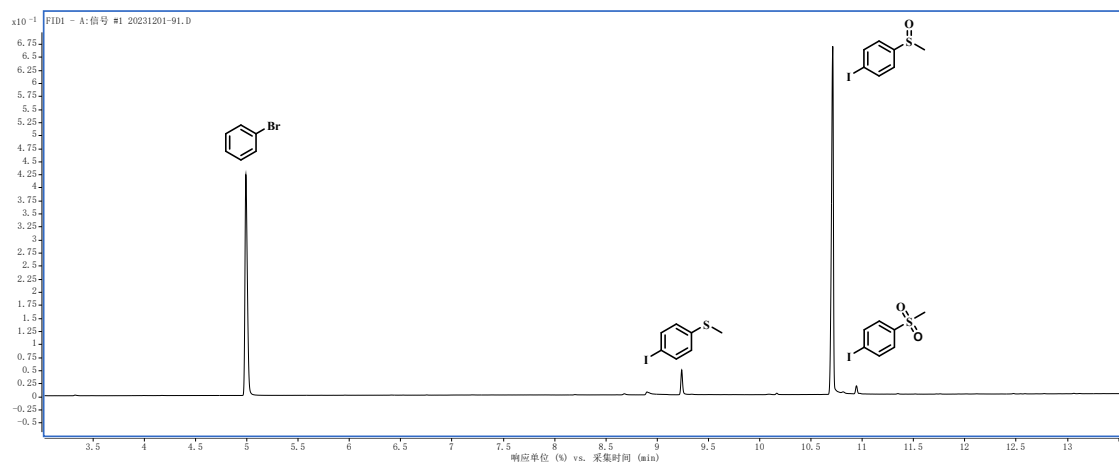


Table 2, Entry 10

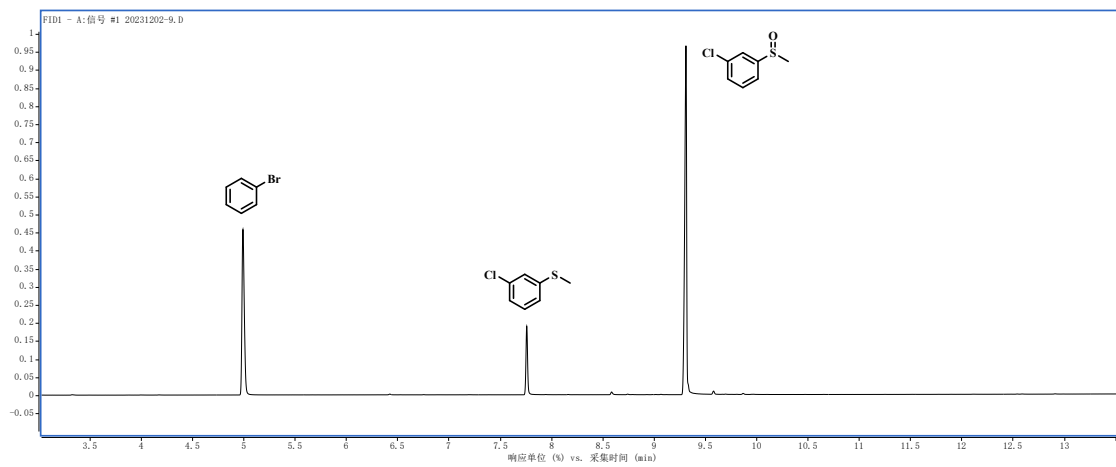


Table 2, Entry 11

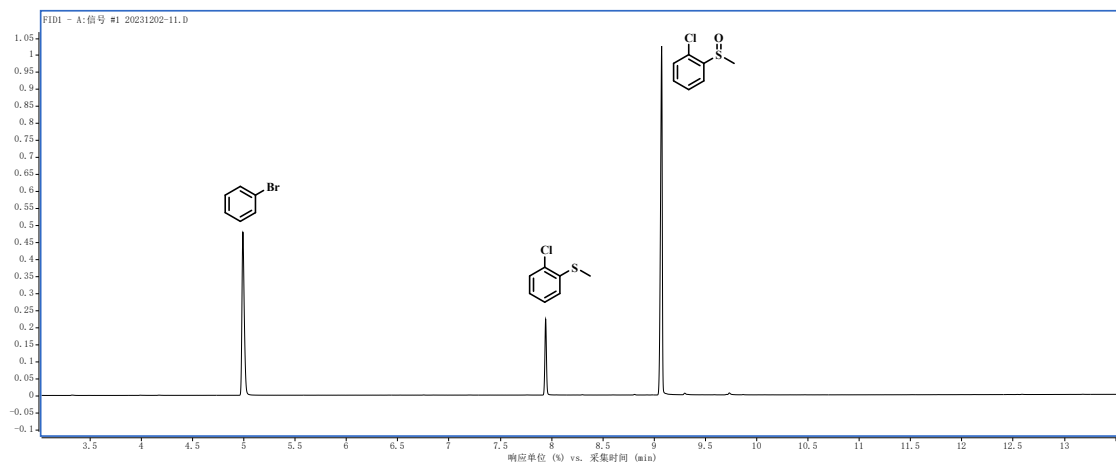


Table 2, Entry 12

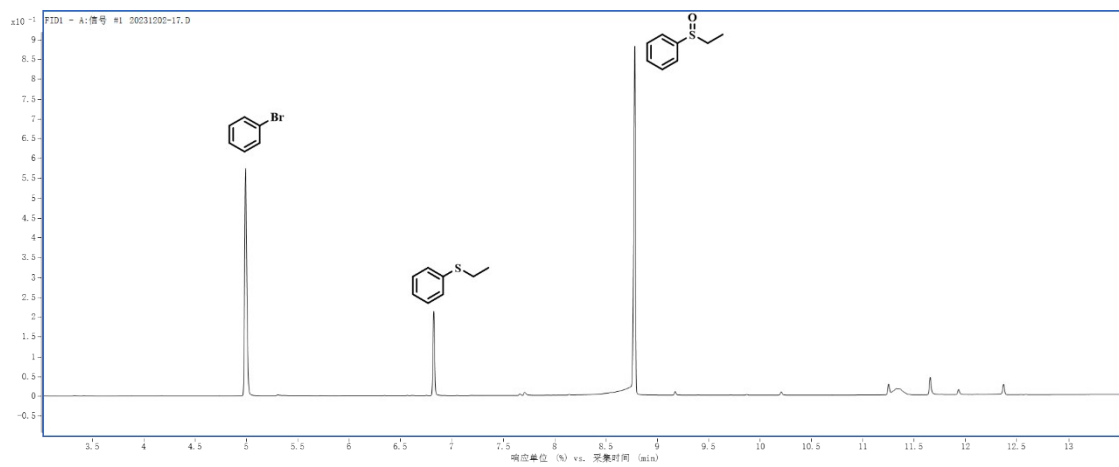


Table 2, Entry 13

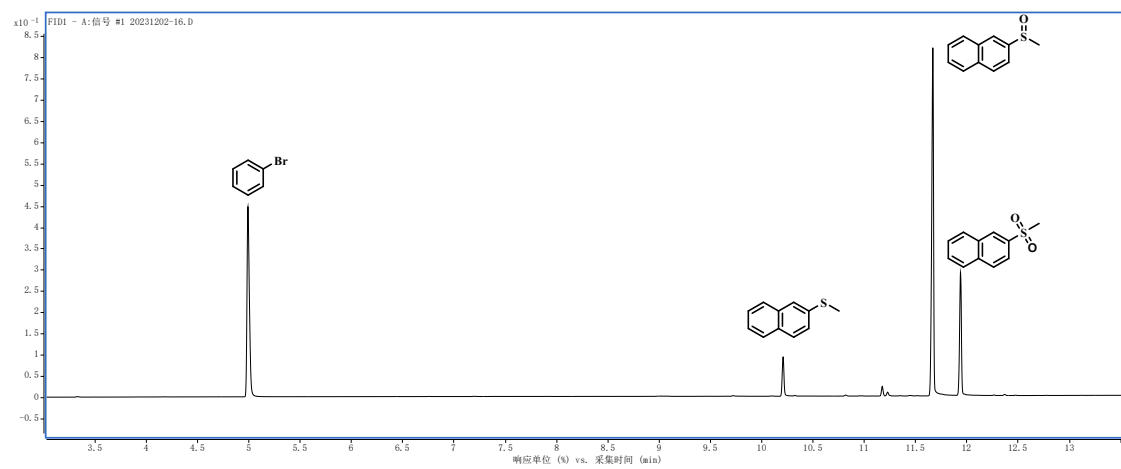
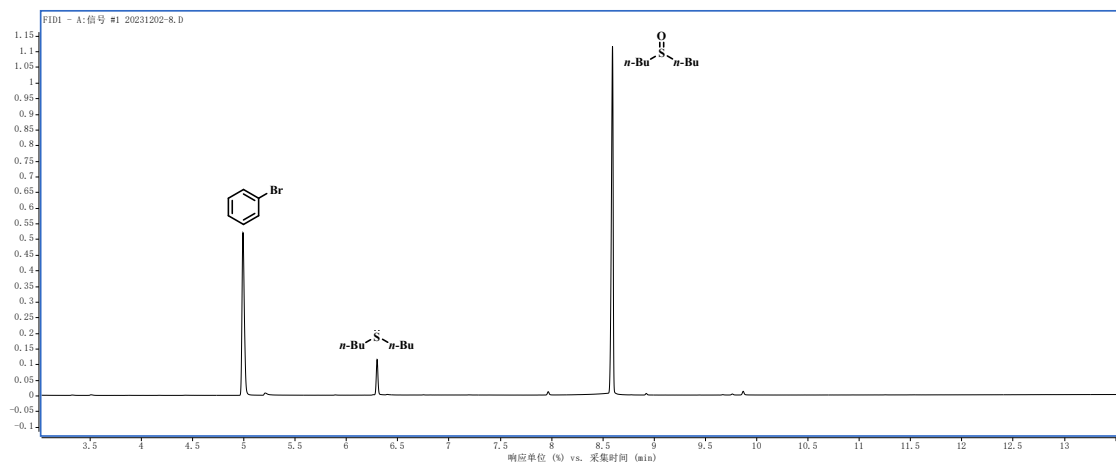


Table 2, Entry 14



## References

1. Q. Li, X. W. Lan, G. Y. An, L. Ricardez-Sandoval, Z. G. Wang and G. Y. Bai, *ACS Catal.*, 2020, **10**, 6664–6675.
2. C. L. Su, R. Tandiana, B. B. Tian, A. Sengupta, W. Tang, J. Su and K. P. Loh, *ACS Catal.*, 2016, **6**, 3594–3599.
3. H. Wang, S. L. Jiang, S. C. Chen, D. D. Li, X. D. Zhang, W. Shao, X. S. Sun, J. F. Xie, Z. Zhao, Q. Zhang, Y. P. Tian and Y. Xie, *Adv. Mater.*, 2016, **28**, 6940–6945.
4. Z. H. Zhao, M. J. Liu, K. Zhou, L. D. Guo, Y. J. Shen, D. Lu, X. Hong, Z. B. Bao, Q. W. Yang, Q. L. Ren, P. R. Schreiner and Z. G. Zhang, *ACS Appl. Mater. Interfaces*, 2023, **15**, 6982–6989.
5. X. J. Lang, W. Hao, W. R. Leow, S. Z. Li, J. C. Zhao and X. D. Chen, *Chem. Sci.*, 2015, **6**, 5000–5005.
6. Z. J. Gu, J. J. Wang, Z. Shan, M. M. Wu, T. T. Liu, L. Song, G. X. Wang, X. H. Ju, J. Su and G. Zhang, *J. Mater. Chem. A*, 2022, **10**, 17624–17632.